Computers & Geosciences 70 (2014) 120–127

Contents lists available at ScienceDirect

Computers & Geosciences

journal homepage: www.elsevier.com/locate/cageo

GEOFIM: A WebGIS application for integrated geophysical modeling in active volcanic regions

Gilda Currenti, Rosalba Napoli *, Antonino Sicali, Filippo Greco, Ciro Del Negro

Istituto Nazionale di Geofisica e Vulcanologia, Sezione di Catania, Osservatorio Etneo, Italy

ARTICLE INFO

Article history:
Received 27 December 2013
Received in revised form
30 April 2014
Accepted 2 May 2014
Available online 11 May 2014

Keywords:
Volcano monitoring
Integrated geophysical modeling
Inverse procedure
Etna volcano

ABSTRACT

We present GEOFIM (GEOphysical Forward/Inverse Modeling), a WebGIS application for integrated interpretation of multiparametric geophysical observations. It has been developed to jointly interpret scalar and vector magnetic data, gravity data, as well as geodetic data, from GPS, tiltmeter, strainmeter and InSAR observations, recorded in active volcanic areas. GEOFIM gathers a library of analytical solutions, which provides an estimate of the geophysical signals due to perturbations in the thermal and stress state of the volcano. The integrated geophysical modeling can be performed by a simple trial and errors forward modeling or by an inversion procedure based on NSGA-II algorithm. The software capability was tested on the multiparametric data set recorded during the 2008–2009 Etna flank eruption onset. The results encourage to exploit this approach to develop a near-real-time warning system for a quantitative model-based assessment of geophysical observations in areas where different parameters are routinely monitored.

1. Introduction

Volcano monitoring involves geophysical techniques that detect magma movements and associated interactions with surrounding rocks and fluids. The ascent of magma to the Earth's surface generates a wide variety of geophysical signals, which can be detected before and during the volcanic eruptions. In particular, ground deformation, gravity and magnetic changes in volcanic areas are generally recognized as reliable indicators of unrest, resulting from the accumulation and intrusion of fresh magma within the shallow rock layers. However, the different geophysical measurements, recorded by the monitoring networks installed in volcanic areas, are generally interpreted separately from each other and the consistency of interpretations coming from different methods is qualitatively checked only "*a posteriori*". Actually, to move towards a model-based assessment of geophysical observations will require integration of different geophysical signals and models. This is probably the most effective procedure able to yield more robust estimates of source parameters and reduce the ambiguity on the range of likely solutions.

The integrated modeling of these geophysical signals could improve our understanding of volcanic processes and our ability to identify renewed volcanic activity, forecast eruptions, and assess hazards. The main purpose of geophysical modeling is the identification of the parameters of volcanic sources producing these observable changes (Currenti et al., 2007, 2011a; Napoli et al., 2008). Here, we present a WebGIS application, called GEOFIM (GEOphysical Forward/Inverse Modeling), which is able to handle a multiple geophysical dataset and perform a quick joint inversion of geophysical signals to define the underlying volcanic source parameters (Fig. 1). In particular, GEOFIM can jointly model magnetic, gravity, and deformation data by trial and errors forward modeling or through an inversion procedure based on genetic algorithm. The careful use of high quality data sets, together with efficient modeling tools, can yield valuable insights into the nature of the volcanic sources. The forward modeling allows to match measured geophysical data to identify a reasonable volcanic source by choosing among different analytical models and source geometries (sphere, ellipsoids and rectangular dislocation). However, as the geophysical models are highly nonlinear and characterized by a high number of parameters, GEOFIM uses a non-linear optimization procedure based on the Non-dominated Sorting Genetic Algorithm (NSGA-II; Deb et al., 2000), which automatically finds the best model parameter that minimizes an objective function, in an iterative way, comparing the observed data with the numerical solutions.

GEOFIM was tested on ground deformation, gravity and magnetic measurements recorded on the onset of 2008–2009 eruption of Mt. Etna (Italy). The modeling results show that the best fit source is coherent with those reported in literature (Napoli et al., 2008; Currenti et al., 2011a, 2011b), proving the potential of

* Corresponding author.
E-mail address: rosalba.napoli@ct.ingv.it (R. Napoli).

http://dx.doi.org/10.1016/j.cageo.2014.05.001
0098-3004/

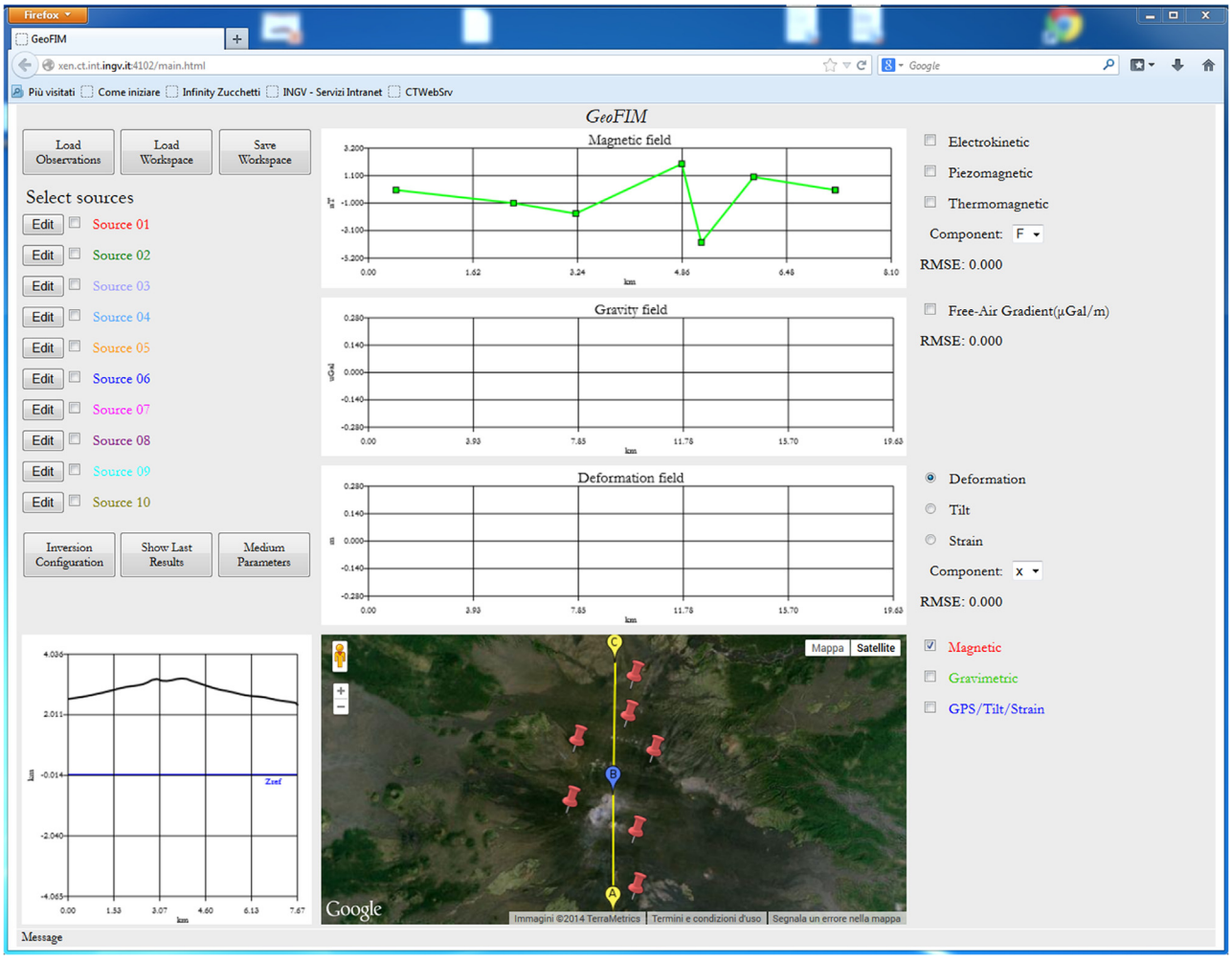

Fig. 1. GEOFIM forward modeling main window.

GEOFIM to interpret different geophysical dataset and to constrain the active magmatic source in near-real-time.

2. Forward models

A key point in the geophysical modeling is the choice of the appropriate forward model relating the magmatic source to the expected geophysical changes recorded by the monitoring networks. Magma ascent to the Earth's surface forces surrounding crustal rocks apart perturbing the thermal and stress state and producing ground deformation and variations in the magnetization and in the density distributions of rocks. Ground deformation produced by ascending magma are usually computed solving the elasto-static equations (Mogi, 1958; Yang et al., 1988). Gravity changes are estimated computing the gravity field engendered by the density redistribution due to arrival of additional mass and deformations of the surrounding rocks (Hagiwara, 1977; Okubo, 1992). Magnetic variations can be attributed to different mechanisms engendered by the perturbation of the stress field, such as piezomagnetic (Sasai, 1986; Utsugi et al., 2000) and electrokinetic effects (Fitterman, 1979; Murakami, 1989), and by changes in the rock magnetization, such as those produced by thermal demagnetization/remagnetization mechanisms. Therefore, in GEOFIM a library of forward models has been implemented to compute the expected geophysical changes using analytical solutions available in literature (Fig. 2). Although analytical models are based on a number of simplifications, they provide a first approximation of the expected geophysical changes for a variety of source geometries. Geophysical changes produced by magma accumulation have been traditionally interpreted by idealized spherical and ellipsoidal sources. Whereas magma intrusion processes are usually represented by opening cracks and/or a rectangular dislocations. For each model a short description, a schematic representation and references to analytical formulations used as computational routines are given below. The list of volcano sources available in GEOFIM is reported in Table 1. The analytical solutions have been compared and validated with numerical solutions performed with Finite Element Method (Currenti et al., 2007, 2008, 2009).

2.1. Spherical model

The simplest way to model the inflation or deflation of a magma chamber at depth is a dilatation point source (Mogi's source), which is quite appropriate to approximate spherical overpressured source when the radius is far smaller than its depth. Therefore, in GEOFIM the general Mogi model (1958) simulating a spherical source embedded in a homogeneous elastic half-space medium was implemented to compute ground deformation generated by pressure changes within the magmatic source. To compute gravity and piezomagnetic changes, which are expected to accompany inflation or deflation of a magma chamber, the analytical solutions devised by Sasai (1986) and Hagiwara (1977) have been used, respectively. For spherical sources no electronkinetic

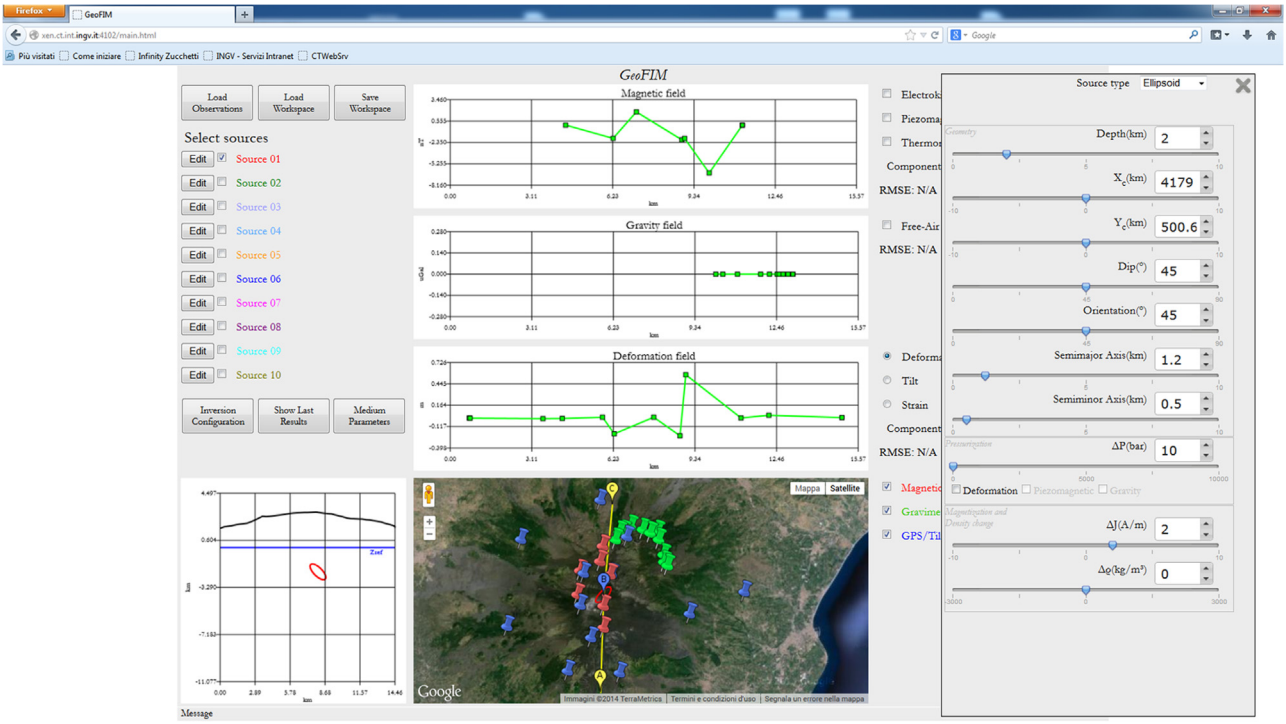

Fig. 2. Prolate ellipsoid source parameters. Section and plane views of the source geometry in GEOFIM

Table 1
List of volcano sources and tectonic dislocations.

Model	Reference		
	Gravity	**Magnetism**	**Ground deformation**
Sphere	Hagiwara (1977) Blakely (1996)	Sasai (1986) Blakely (1996)	Mogi (1958)
Prolate ellipsoid	Clark et al. (1986)	Clark et al. (1986)	Yang et al. (1988)
Dislocation	Okubo (1992)	Utsugi et al. (2000) Murakami (1989)	Okada (1992)
Rectangular prism	Okubo and Watanabe (1989)	Blakely (1996)	

variations are expected due to the isotropy of the source. Measurable electrokinetic variation is expected to occur when the radial symmetry is destroyed and the greater component of this field is orientated parallel to the strike of the anisotropy structure (Fitterman, 1979; Murakami, 1989). Moreover, gravity changes related to the density variations of the source due to mass input and magnetic variations due to rock magnetization changes are computed using solutions reported in Blakely (1996). These solutions consider density and magnetization contrasts between the source and the embedding medium.

2.2. Prolate ellipsoid model

GEOFIM also provides the solutions for prolate ellipsoids, which allow to describe more realistically volcanic sources thanks to the higher number of geometry parameters. The geometry is suitable to represent both magma chambers and elongated volcanic conduits. GEOFIM uses Yang et al. (1988) solutions, with corrections reported in Newmann et al. (2006), for a pressurized dipping prolate ellipsoid for computing the ground deformation. Clark et al. (1986) solutions are implemented for computing gravity and magnetic variations due to density and magnetization changes within the ellipsoidal source.

2.3. Rectangular dislocation model

Dislocation source leading to ground deformation and gravity changes can be modeled in GEOFIM through the sets of analytical expressions devised by Okada (1992) and Okubo (1992), respectively. Both analytical formulations account for the effects arising from dislocations buried in a homogeneous half-space and, while the former allows to calculate the displacement, stress and strain fields due to the faulting processes, the latter allows to calculate all the contributions to the corresponding gravity changes. Parallel, a piezomagnetic model, based on the analytical formulation described in Utsugi et al. (2000), who revised solutions given in Sasai (1991), was adopted to calculate the expected piezomagnetic field changes at the earth's surface for a rectangular dislocation. Dip-slip, strike-slip and tensile-opening dislocations with arbitrary dip and strike angles can be considered. Also the electrokinetic effect expected at the ground surface was computed by using the Murakami (1989) formulation, which provides the analytical solutions for computing magnetic fields due to an inclined rectangular dislocation separating two media with different streaming potential coefficients. Moreover, the expected gravity and magnetic changes produced by density and magnetization variations within a rectangular prism are calculated using the analytical solution reported in Blakely (1996).

2.4. Inversion problem

The inverse method combines forward models with appropriate optimization algorithms to automatically find out the best model parameters (Beauducel and Cornet, 1999; Owen et al., 2000; Tiampo et al., 2004; Carbone et al., 2006; Currenti et al., 2007; Battaglia et al., 2013). As a rule, geophysical inverse problems are ill-posed, suffering from the ambiguity and instability of inverse solutions. Because of the inherent non-uniqueness of the inverse problems, there are infinite sources that could explain the observed geophysical data within the error limits. Moreover, the geophysical inverse problems are usually unstable. Small variations in the observed data may result in dramatic changes of the model parameters. Integrated inversions of multiparametric data have the potential to yield more robust estimates of source parameters and reduce the ambiguity or the range of likely solutions (Currenti et al., 2007). The aim of the multiparametric inversion is to find the vector of model parameters $m = \{m_1, \ldots, m_p\} \in \boldsymbol{M}$ that minimizes the misfit between the observed and calculated data ($\boldsymbol{M}$ is the model space). The joint inversion of different geophysical observables implies that the misfits for each i-th dataset are simultaneously minimized:

$$f_i(\mathbf{m}) = ||g_i(\mathbf{m}) - d_i^{obs}|| \quad i = 1, \ldots, k \tag{1}$$

where f_i is an objective function and denotes the difference between the value calculated through $g_i(\boldsymbol{m})$ (forward model) and the observed value d_i^{obs} for each i-th geophysical observable. Therefore, the joint inversion of a multiparametric geophysical dataset can be regarded as a *multiobjective optimization problem* (MOP). To solve this problem means to find the set of model parameters $\boldsymbol{m}^*$ that satisfies some constraints and optimizes the objective function vector, whose elements are the objective functions:

$$\begin{aligned} &\boldsymbol{m}^* = \min_{m \in M} \boldsymbol{F}(\mathbf{m}) \quad \text{with} \quad m_j^{min} \le m_j \le m_j^{max} \quad j = 1, \ldots, p \\ &\text{where} \quad \boldsymbol{F}(\mathbf{m}) = [f_1(\mathbf{m}), f_2(\mathbf{m}), \ldots, f_k(\mathbf{m})] \end{aligned} \tag{2}$$

Since the $g_i(\boldsymbol{m})$ forward models are non-linear operators, it calls for using robust non-linear inversion methods. Among several techniques, multi-objective Genetic Algorithms (GAs) have been proven to be a robust global search procedure suitable for nonlinear and multimodal inverse problems (Davis, 1996), which are typically encountered in geophysics (Currenti et al., 2005; Carbone et al., 2008; Beauducel and Cornet, 1999). In the framework of multi-objective Genetic Algorithms, the estimate obtained through minimization of Eq. (2) represents a Pareto optimal solution (Fonseca and Fleming, 1993; Deb and Gupta, 2005; Sobol, 1985). Although the joint inversion of multi-parametric geophysical data is not a problem with highly contradictory objectives, it is unlikely that the same set of model parameters is the best for all the objectives. That is caused by the natural uncertainty (noise) that affects the data and, generally, the limited number of available measurements. Hence, any Pareto optimal solution is the result of a trade-off made between the objectives. GAs based on the Pareto approach (Deb et al., 2000) were developed, which differ from other similar inversion schemes mainly in the population sorting procedure. The latter is based on the non-dominance concept: a solution $\boldsymbol{m}_1$ is said not to be dominated by $\boldsymbol{m}_2$ if the following two conditions are satisfied:

$$\begin{aligned} &1.\quad f_i(\boldsymbol{m}_1) \le f_i(\boldsymbol{m}_2) \quad \text{for } i = 1, \ldots, k \\ &2.\quad f_i(\boldsymbol{m}_1) < f_i(\boldsymbol{m}_2) \quad \text{for at least one } i \end{aligned} \tag{4}$$

A solution $\boldsymbol{m}^*$ is said to belong to the Pareto optimal set P if and only if no other $\boldsymbol{m} \in \boldsymbol{M}$ exists such that $f_i(\boldsymbol{m}) \le f_i(\boldsymbol{m}^*)$, for all $i = 1, \ldots, k$ and $f_i(\boldsymbol{m}) \ne f_i(\boldsymbol{m}^*)$ for at least one i. In other words, $\boldsymbol{m}^*$ is a Pareto optimal solution if there exists no feasible solution $\boldsymbol{m}$ that would decrease some criterion without causing a simultaneous increase in at least one other objective function. The set of the objective function vectors, whose solutions are in the Pareto optimal set, forms the Pareto front.

The NSGA-II algorithm (Non-dominated Sorting Genetic Algorithm), devised by Deb et al. (2000), classifies the population of possible solutions into several sets of non-domination levels (Deb et al., 2002). A rank is assigned to each solution depending on the non-domination level to which it belongs (Deb et al., 2000). Obviously, non-dominated solutions of the first-level are candidates for Pareto-optimal solutions. Besides the ranking procedure, the population is evolved using well-known GA operations (selection, crossover and mutation operators on real numbers). The use of NSGA-II algorithm in GEOFIM has two main advantages. Firstly, no scalarization is required to transform the MOP into a single one objective problem (Schwarzbach et al., 2005; Carbone et al., 2008). Secondly, in a single run of inversion, GEOFIM provides a set of solutions (instead of a single one as in traditional approaches) underlining the inherent ambiguity of geophysical inversions and giving a representation of it through the Pareto front. It makes possible to understand whether the objectives "cooperate" (have similar optimal solutions) or "conflict" (have different optimal solutions) with each other. By investigating the distribution of the objectives in the vector space, it is possible to understand whether multiple inverse solutions, each able to satisfactorily match a family of geophysical observations, are likely to occur. That provides a depiction of the trade-off between competing objectives and thus allows to better quantify the ambiguity of the inverse solutions.

2.5. Features and capabilities

GEOFIM has been developed using a WebGIS-based system that integrates geophysical models and WebGIS techniques. It is based on a client/server architecture. The server side is implemented in C++ programming language and uses the TCP/IP protocol to establish communication with the client. The client side is designed in HTML5 and JavaScript languages and exploits the WebSocket protocol, the jQuery library and Google Maps API v3. The WebSocket provides a major advance for a real-time communication between the client and the server. The jQuery library is used mainly to support the interface design and interaction. Google Maps API offers all the necessary interface features for a smooth and efficient navigation over maps. GEOFIM enables managing observed gravity, magnetic and deformation data, source models, and calculations into a highly interactive framework. Geophysical observations are easily imported from one or more datasets loading simple text files (containing information about station position and available data). In particular, magnetic data from scalar and vector magnetometers and gravity data from relative and absolute gravimeters can be imported. Also geodetic data from GPS, tiltmeter and strainmeter ground-based monitoring stations as well as InSAR data from satellite observations can be read. The source model can be set up as one or a set of discrete solid bodies such as sphere, ellipsoid, and prism. Both observation points and sources are visualized using Google Maps in the Universal Transverse Mercator (UTM, WGS84 ellipsoid) coordinates and are shown in a plane view and in a profile window chosen by the user. GEOFIM quickly performs the calculation of the anomalies generated by the volcanic sources, allowing the user to choose different models and to superimpose their effects up to ten sources at the same time. The geophysical observations and the computed fields are simultaneously visualized in three windows showing the ground deformation, gravity and magnetic fields with an estimate of the fit by means of the Root Mean Square Error (RMSE) values. GEOFIM offers a dedicated window in order to set the density and the elastic, electrokinetic and

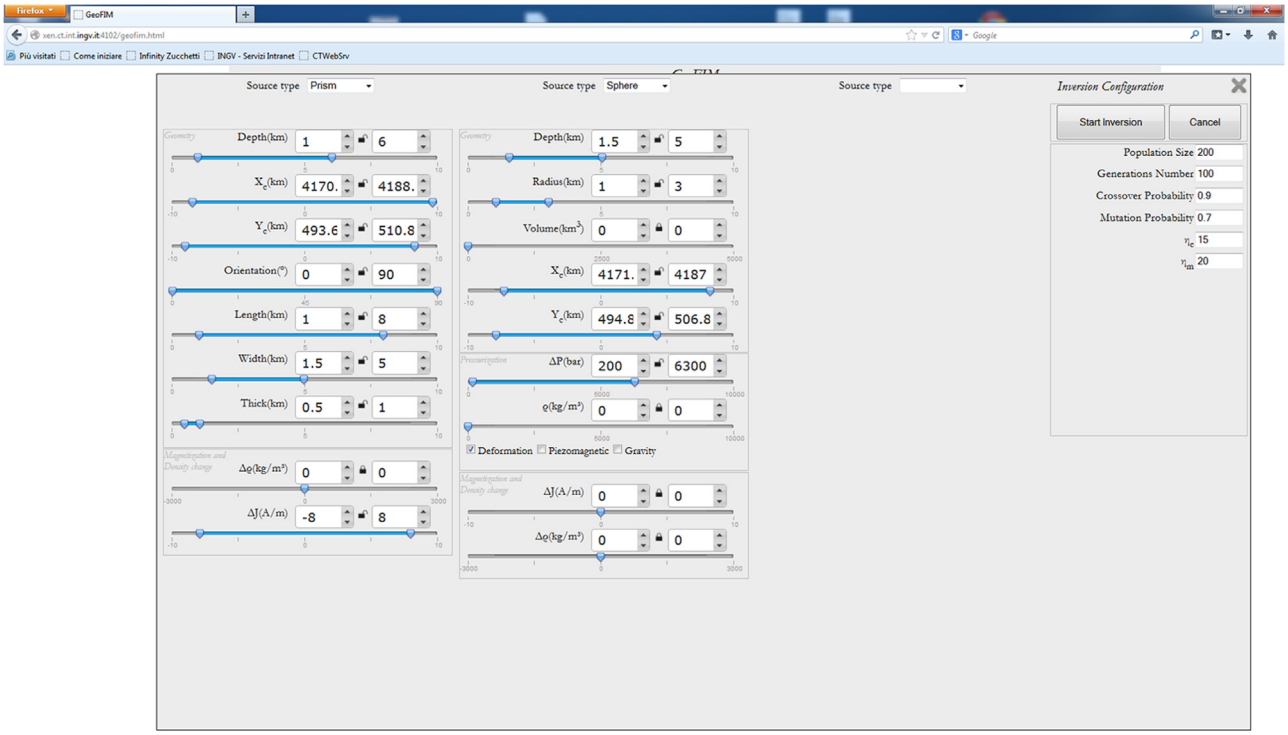

Fig. 3. GEOFIM inversion configuration window. Source parameters and NSGA-II algorithm set-up can be chosen by the users.

magnetic parameters of the medium, and the source parameters involved in computational routines. Forward and inversion procedures can be chosen to calculate the expected geophysical changes. Forward modeling takes place when source and/or medium parameters are manually adjusted by the users through sliders in order to improve the fit between the observed and the calculated fields due to the chosen models. The real-time calculation and visualization of the modeling results allows the user to have immediately an estimate about the influence of model parameters in the geophysical signals. The user can also enter a particular value in a textbox allowing a fine-tuning when performing a trial and error adjustment, or when using a known solution. In the inversion procedure GEOFIM automatically adjusts the model parameters to minimize the misfit between the observations and model computations. Fig. 3 shows the inversion configuration set-up. The text box on the right allows to define typical NSGA-II parameters. GEOFIM looks for up to three sources whose combined effects match the observed signals. For each source it is possible to invert for deformation, gravity and magnetic fields separately, as well as to combine them. At the end of the inversion the Pareto front is also shown allowing to select one of the optimal solutions. At the same time, misfit between observed and calculated values for every objective function is shown as well as solution parameters. Finally, for the selected solution an immediate comparison between observed and calculated values is provided. The demonstration version of GEOFIM is available on the Web at http://ufgm.ct.ingv.it/geofim/geofim.html.

2.6. 2008–2009 Eruption at Etna volcano

The capability of GEOFIM to handle a multiple geophysical dataset and perform a joint inversion of geophysical signals was validated on data set collected during the 2008–2009 Etna eruption. The onset of this eruptive activity was accompanied by remarkable changes in the local magnetic field and by significant ground deformation recorded by continuously running stations. In particular, large negative changes in local magnetic field, ranging between −1.8 and −6.5 nT, occurred at the stations placed on the summit area of the volcano (Napoli et al., 2008). Simultaneously, GPS network recorded horizontal displacements of a few tens of centimetres at the summit stations, whereas smaller variations were observed at the stations sited in the middle flanks. In close temporal coincidence with these geophysical changes a superficial seismic swarm started from the eastern base of the summit craters and in a few hours the earthquakes propagated toward the northern flank. A dry fracture field formed on the northern flank of the volcano and an E-W eruptive fissure opened in the upper sides of the Valle del Bove (Napoli et al., 2008; Currenti et al., 2011b). The trial and error forward modeling of these data using different analytical solutions (Napoli et al., 2008) pointed to a shallow intrusion propagating laterally to the NNW direction from the central conduit driven by a magmatic overpressure.

Table 2
Search range for the dislocation model parameters. The coordinates are in UTM-WGS84 projection. Parameters for the piezomagnetic dislocation source modeling the deformation and magnetic data recorded during the onset of 2008–2009 Etna eruptive activity. The standard deviation of each parameter is computed over 50 different runs of GA.

Fault model parameters	Ranges	Obtained parameters	Standard deviation
δ, dip fault	0–90°	88°	2.71°
α, azimuth (from North)	0–180°	−22°	2.91°
D, depth	50–1000 m	101 m	216.5 m
W, fault width	200–5000 m	1000 m	556.2 m
L, fault length	500–6000 m	2180 m	730.8 m
Ut, tensile opening	0.1–3 m	2 m	0.17 m
Xc, North coordinate	4175–4185 km	4179 km	135.31 m
Yc, East coordinate	498–504 km	500.680 km	159.02 m

Exploiting the NSGA-II optimization procedure embedded within GEOFIM, an integrated geophysical inversion of the available dataset was formulated, under the following "*a priori*" assumptions:

1. A tensile source lies within the zone of the seismic swarm accompanying the magma propagation;
2. The top depth of the tensile source is expected to be very shallow since it is supposed to be closely related to the fracture field developed in the northern flank of the volcano;
3. Since gravity survey carried out in May 2008 along the North-East Rift did not cover the summit area of the volcano where the fracture field developed, no significant variations were recorded. Therefore, these data does not add constrain to the model and are disregarded in the inversion.

Table 3
The magneto-elastic parameters estimated in the upper crust on Mt. Etna.

Magneto-elastic parameters	Symbol	Value
Average magnetization	J	2 A/m
Curie depth	H	15,000 m
Magnetic inclination	I	53°
Magnetic declination	D	2°
Rigidity	μ	30 GPa
Stress sensitivity	β	0.0001 bar^{-1}

Hence, we invert ground deformation and magnetic data to infer the position and the geometrical parameters of the tensile source leading to the geophysical changes. The dislocation model involves eight parameters: $m=\{$Dip, Orientation, Depth, Width, Length, Ut, Xc, Yc$\}$, whose descriptions and search ranges are reported in Table 2. The NSGA-II was requested to determine the best solution for the dislocation parameters in the search space. The values of the parameters of the magneto-elastic medium used

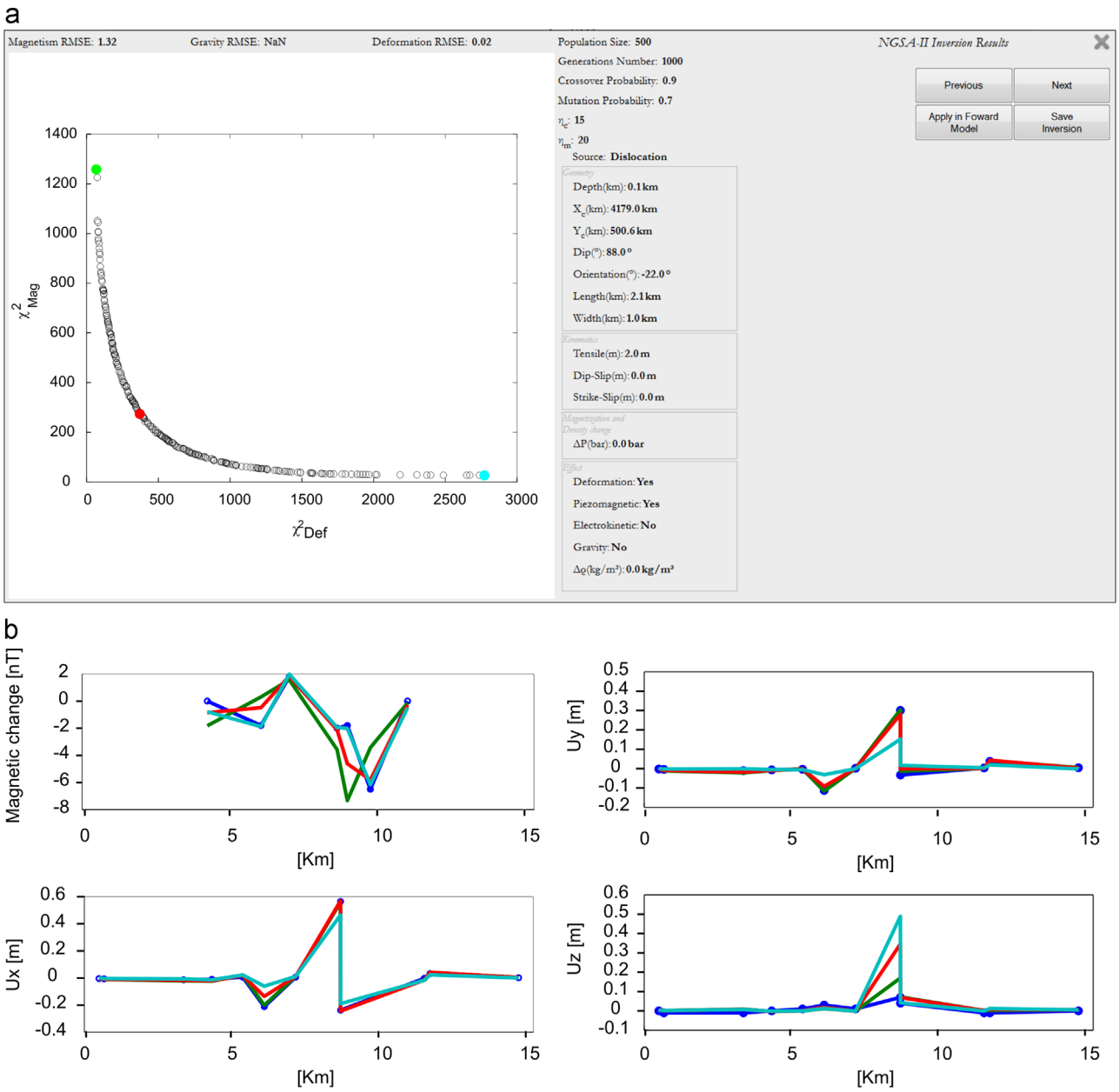

Fig. 4. Inversion modeling results window (a). The data misfits are shown for the Pareto front. The NSGA-II parameters and the retrieved source are also reported. Observed (line-dots) and computed (lines) magnetic and deformation fields (b). The three computed fields (colored lines) refer to the three solutions in the Pareto front (colored dots). (For interpretation of the references to color in this figure legend, the reader is referred to the web version of this article.)

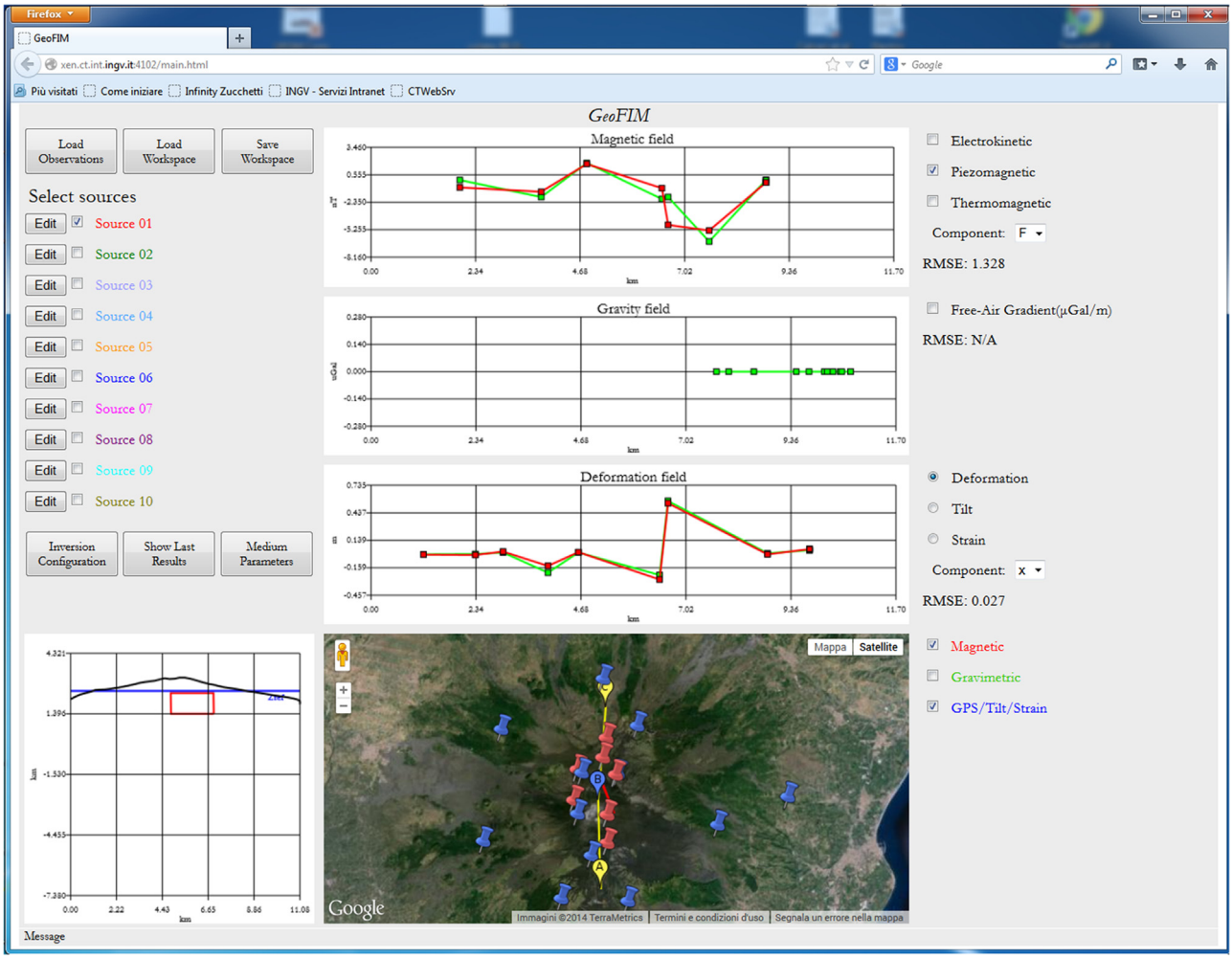

Fig. 5. Integrated geophysical model obtained by GEOFIM for the magmatic intrusion occurred during the 2008–2009 Etna eruption. Observed (green) and calculated (red) fields are shown in the different windows. The RMSE between data and computed solutions are also reported. Plane and cross-section views of the tensile source are shown at the bottom. (For interpretation of the references to color in this figure legend, the reader is referred to the web version of this article.)

in these calculations are shown in Table 3. The rock magnetization of 2 A/m was estimated from surface samples near the various magnetometer sites (Del Negro and Napoli, 2002). The Lamé's constants were set up to $\lambda=\mu=30$ GPa that leads for Poisson's ratio of 0.25, a reasonable approximation to the values estimated in the upper crust on Mt. Etna.

The convergence of the NSGA-II algorithm depends on the control parameters, explicitly (i) the size of the initial population; (ii) the crossover probability Pc; and (iii) the mutation probability Pm (Deb et al., 2000). A large number of initial individuals ensures more possibilities to explore the overall parameter space but makes the inversion procedure more time-consuming. High values for the crossover and mutation probabilities guarantee a fine exploitation and exploration, respectively, but decrease the rate of convergence toward the solution that minimizes the objective function. Initial tests suggested a crossover probability Pc of about 0.9 and Pm of about 0.7, which seem to be a good compromise between exploration and exploitation as well as between efficiency and computation time (Deb, 2001). We run 1000 generations, using an initial population of 500 individuals. The number of iterations was sufficient to assure a good convergence of the algorithm. Additional tests showed that increasing the number of iterations does not lead to improvements in the objective function vector, composed of the two χ^2 values on the misfit between model computations and observations for the deformation and magnetic fields:

$$\chi_i^2 = \sum_n \frac{(g_n - d_n^{obs})^2}{\sigma_n^2} \tag{5}$$

where σ_n^2 is the standard deviation of each measurements, which is of 0.005 m for the horizontal deformation components, 0.05 m for the vertical deformation components, and 0.2 nT for the magnetic field (Currenti et al., 2011a). Through the NSGA-II algorithm, a family of solutions is achieved, whose Pareto front is shown in Fig. 4a. Among the several techniques that have been developed to properly choose the best-fit solution in multi-objective inverse problems, we used the L-curve criterion, which selects the solution in correspondence of the point of maximum curvature (red dot) to find a trade-off between minimizing the two dataset misfits. The computed magnetic changes and deformation field for the best-fit tensile source, whose parameters are reported in Table 2, agree well with the observations with a RMSE of 1.32 nT for the magnetic field and 0.02 m for the deformation field (Fig. 4b). GEOFIM allows also to explore all the solutions in the Pareto front. The solution (cyan dot), which better suits the magnetic data, deteriorates the fit with the deformation data (Fig. 4b). On the other hand, the solution (green dot), which better suits the deformation data, worsen the fit with the magnetic data (Fig. 4 b).

3. Conclusion

The ever-expanding use of geophysical monitoring techniques of volcanoes generates multidisciplinary time-series of data, which require integrated modeling procedures for assessing whether magma accumulation and migration could actually lead to an eruption. With the aim of performing this integration, we developed the WebGIS application GEOFIM, which is able to model simultaneously magnetic, gravity and deformation data gathered in active volcanic areas featuring a user-friendly graphical interface. The joint interpretation can be performed by trial and errors forward modeling or through an inversion procedure based on the NSGA-II, which is particularly suitable to globally optimize highly non-linear problems. In active volcanoes, where different geophysical parameters are routinely monitored, multi-objective evolutionary algorithms prove to be a powerful tool to jointly invert multi-method geophysical data and lead to important insights into the active magmatic sources.

GEOFIM was validated on the multidisciplinary data set recorded during the onset of the 2008–2009 Etna flank eruption. The simultaneous inversion of magnetic and geodetic measurements provides a coherent interpretation of the observations and allows delineating the magma intrusion process occurred in the northern flank of the volcano (Fig. 5). Although the model is based on simplified elastic half-space medium assumption disregarding the effects of topography and medium heterogeneity that could affect the modeling results (Currenti et al., 2009, 2011a,2011b), GEOFIM quickly provides a first-order estimation of source characteristics leading to constraints on location, depth, volume, mass and overpressure. Distinguishing these features is crucial for a deeper understanding of the ongoing volcano activity.

Summing up, the user-friendly WebGIS application of GEOFIM allows to quickly invert jointly different geophysical data constraining magma accumulation and intrusion in volcanic areas. By considering integrated dislocation models (Okada, 1992; Okubo, 1992; Utsugi et al., 2000) GEOFIM may be also used to identify the main structures activated during a seismic crisis in active tectonic region. This could allow to track the evolution of the ongoing activity providing a scenario that could be useful for hazard assessment. The exploitation of this approach could pose the basis for a next generation of near-real-time warning system, moving from anomaly detection toward a quantitative model-based assessment of geophysical observations.

Acknowledgments

This work was developed within the framework of TecnoLab, the Laboratory for Technological Advance in Volcano Geophysics organized by INGV-CT, DIEES-UNICT, and DMI-UNICT. We are grateful to the Editor in-Chief Jef Caers, Fabio Caratori Tontini and an anonymous reviewer for their helpful comments.

References

Battaglia, M., Cervelli, P.F., Murray, J.R., 2013. dMODELS: a MATLAB software package for modeling crustal deformation near active faults and volcanic centers. J. Volcanol. Geotherm. Res. 254, 1–4 http://dx.doi.org/10.1016/j.jvolgeores.2012.12.018.

Beauducel, F., Cornet, H.F., 1999. Collection and three-dimensional modeling of GPS and tilt data at Merapi volcano, Java. J. Geophys. Res. 104 (B1), 725–736.

Blakely, R.J., 1996. Potential Theory in Gravity and Magnetic Applications. Cambridge University Press, Cambridge (437 pp.).

Carbone, D., Currenti, G., Del Negro, C., 2006. Elastic model for the gravity and elevation changes prior to the 2001 eruption of Etna volcano. Bull. Volcanol. 69, 553–562, http://dx.doi.org/10.1007/s00445-006-0090-5.

Carbone, D., Currenti, G., DelNegro, C., 2008. Multi-objective genetic algorithm inversion of ground deformation and gravity changes spanning the 1981 eruption of Etna volcano. J. Geophys. Res. 113, B07406, http://dx.doi.org/10.1029/2006JB004917.

Clark, D.A., Saul, S.J., Emerson, D.W., 1986. Magnetic and gravity anomalies of a triaxial ellipsoid. Explor. Geophys. 17, 189–200.

Currenti, G., Del Negro, C., Nunnari, G., 2005. Inverse modelling of volcanomagnetic fields using a genetic algorithm technique. Geophys. J. Int. 163, 403–418.

Currenti, G., Del Negro, C., Ganci, G., 2007. Modelling of ground deformation and gravity fields using finite element method: an application to Etna volcano. Geophys. J. Int. 169, 775–786, http://dx.doi.org/10.1111/j.1365-246X.2007.03380.x.

Currenti, G., Del Negro, C., Ganci, G., Scandura, D., 2008. 3D numerical deformation model of the intrusive event forerunning the 2001 Etna eruption. Phys. Earth Planet. Inter. 168, 88–96, http://dx.doi.org/10.1016/j.pepi.2008.05.004.

Currenti, G., Napoli, R., Di Stefano, A., Greco, F., Del Negro, C., 2011. 3D integrated geophysical modeling for the 2008 magma intrusion at Etna: Constraints on rheology and dike overpressure. Phys. Earth Planet. Int. 185, 44–52, http://dx.doi.org/10.1016/j.pepi.2011.01.002.

Currenti, G., Napoli, R., Del Negro, C., 2011b. Toward a realistic deformation model of the 2008 magmatic intrusion at Etna from combined DInSAR and GPS observations. Earth Planet. Sci. Lett. 312, 22–27.

Currenti, G., Del Negro, C., Di Stefano, A., Napoli, R., 2009. Numerical simulation of stress induced piezomagnetic fields at Etna volcano. Geophys. J. Int. 179 (2009), 1469–1476, http://dx.doi.org/10.1111/j.1365-246X.2009.04381.x.

Davis, L., 1996. Handbook of Genetic Algorithms. International Thomson Computer Press, London.

Deb, K., Agrawal, S., Pratap, A., Meyerivan, T., 2000. A fast elitist nondominated sorting genetic algorithm for multi-objective optimization: NSGA-II. Kanpur Genetic Algorithms Laboratory (KanGAL), Kanpur, India (Technical Report 2000001).

Deb, K., 2001. Multi-Objective Optimization Using Evolutionary Algorithms. Wiley, Chichester.

Deb, K., Zope, P., Jain, A., 2002. Distributed computing of Pareto optimal solutions using multi-objective evolutionary algorithms. Kanpur Genetic Algorithms Laboratory (KanGAL), Kanpur, India (Technical Report 2002008).

Deb, K., Gupta, H., 2005. Searching for Robust Pareto-Optimal Solutions in Multi-objective Optimization, Lecture Notes in Computer Science. Springer, Berlin/ Heidelberghttp://dx.doi.org/10.1007/b106458.

Del Negro, C., Napoli, R., 2002. Ground and marine magnetic surveys of the lower eastern flank of Etna volcano (Italy). J. Volcanol. Geotherm. Res. 114 (3–4), 357–372.

Fitterman, D.V., 1979. Theory of electrokinetic magnetic anomalies in a faulted half space. J. Geophys. Res. 84, 6031–6040.

Fonseca, C.M., Fleming, P.J., 1993. Genetic algorithms for multi-objective optimization: formulation, discussion and generalization. In: Forrest, S. (Ed.), Genetic Algorithms: Proceedings of the Fifth International Conference. Morgan Kaufmann, San Mateo, CA.

Hagiwara, Y., 1977. The Mogi model as a possible cause of the crustal uplift in the eastern part of Izu Peninsula and related gravity change. Bull. Earthq. Res. Inst., Univ. Tokyo 52, 301–309.

Mogi, K., 1958. Relations between the eruptions of various volcanoes and the deformation of the ground surfaces around them. Bull. Earthq. Res. Inst. 38, 99–134.

Murakami, H., 1989. Geomagnetic Fields produced by electrokinetic sources. J. Geomag. Geoelctr. 41, 221–247.

Napoli, R., Currenti, G., Del Negro, C., Greco, F., Scandura, D., 2008. Volcanomagnetic evidence of the magmatic intrusion on 13th May 2008 Etna eruption. Geophys. Res. Lett. 35, L22301, http://dx.doi.org/10.1029/2008GL035350.

Newmann, A.V., Dixon, T.H., Gourmelen, N., 2006. A four-dimensional viscoelastic deformation model for Long Valley Caldera, California, between 1995 and 2000. J. Volcanol. Geotherm. Res. 150, 244–269.

Okada, Y., 1992. Internal deformation due to shear and tensile faults in a half-space. Bull. Seismol. Soc. Am. 82 (2), 1018–1040.

Okubo, S., Watanabe, H., 1989. Gravity changes caused by a fissure eruption. Geophysical research letters 16 (5), 445–448.

Okubo, S., 1992. Gravity and potential changes due to shear and tensile faults in a half-space. J. Geophys. Res. 7 (B5), 7137–7144.

Owen, S., Segall, P., Lisowski, M., Miklius, A., Denlinger, R., Sako, M., 2000. Rapid deformation of Kilauea Volcano: Global Positioning System measurements between 1990 and 1996. J. Geophys. Res. 105, 18,983–18,998.

Sasai, Y., 1986. Multiple tension-crack model for dilatancy: surface displacement, gravity and magnetic change. 61. Bull. Earthq. Res. Inst., Univ. Tokio, pp. 429–473.

Sasai, Y., 1991. Tectonomagnetic modeling on the basis of the linear piezomagnetic effect. Bull. Earthq. Res. Inst. Univ. Tokyo 66, 585–722.

Schwarzbach, C., Borner, R., Spitzer, K., 2005. Two-dimensional inversion of direct current resistivity data using a parallel, multi-objective genetic algorithm. Geophys. J. Int. 162, 685–695, http://dx.doi.org/10.1111/j.1365-246X.2005.02702.x.

Sobol, I.M., 1985. Multicriteria Interpretation of Method of Regularization of Ill-posed Problems. Preprint of Institute of Applied Mathematics. Academy of Sciences of the USSR, Moscow.

Tiampo, K.F., Fernandez, J., Jentzsch, G., Charco, M., Rundle, J.B., 2004. New results at Mayon, Philippines, from a joint of gravity and deformation measurements. Pure Appl. Geophys. 161, 1433–1452.

Utsugi, M., Nishida, Y., Sasai, Y., 2000. Piezomagnetic potentials due to an inclined rectangular fault in a semi-infinite medium. Geophys. J. Int. 140, 479–492.

Yang, X.M., Davis, P.M., Dieterich, J.H., 1988. Deformation from inflation of a dipping finite prolate spheroid in an elastic half-space as a model for volcanic stressing. J. Geophys. Res. 93 (B5), 4249–4257.